Solution of two dimensional Laplace equation

Assignment 01

Submitted By: Shadman Shahid
Student ID: 0421062311

Submitted To: Dr. Md Shah Alam
Professor Department of Electrical and Electronic Engineering
Bangladesh University of Engineering and Technology

August 2, 2026

1 Problem Statement

Statement of the Problem: *Solve the two-dimensional Laplace's equation of the following form using the finite element method:*

$$\epsilon_{xj}\frac{\partial^2\phi_j(x,y)}{\partial x^2}+\epsilon_{yj}\frac{\partial^2\phi_j(x,y)}{\partial y^2}=0$$

where ϵ_{xj} and ϵ_{yj} are the relative permittivities in the x and y directions, respectively, of electrically anisotropic substrate of j-th region and they are same for isotropic material in the structure. Show the potential distribution over the cross section of the microstrip line of Fig. 1, use 5 V (DC) on the strip.

$W = 0.01$ mm, $T = 0.003$ mm, $h_1 = 0.1$ mm, $h_2 = 2.0$ mm, $l = 1.2$ mm, $\epsilon_r = 12.9$

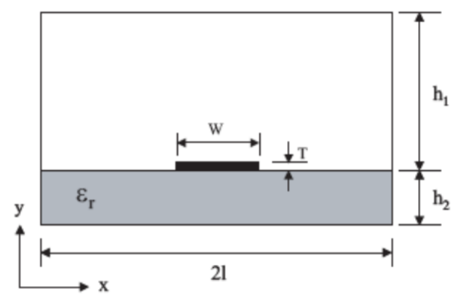

Figure 1: Cross section of a shielded microstrip line.

Figure 1

- Also show the vector electric field over the cross-section.
- Construct a coupled microstrip line with $l = 1.6$ mm and horizontal separation between the strips be $d = 0.012$ mm. All other dimensions remain the same. Apply +5 V and -5 V on the strips. For this coupled microstrip line, show the potential and electric field distribution

Task 1

Methodology

Domain discretization and definition

The structure as defined in the problem statement, can be divided into two regions, considering the metal microstrip to be outside the simulation domain, since the potential across it is already known to be 5 V. The two regions are $F1$ - below the microstrip, and $F2$ above the microstrip. These two sub-domains need to be solved. As per available information, we have an inner boundary condition of 5 V at the edges E1 - - E3 and E5 surrounding the microstrip. This boundary is termed as inner boundary. While the remaining outer boundaries are all set to zero. Thus the Dirichlet boundary conditions in our structure are defined.

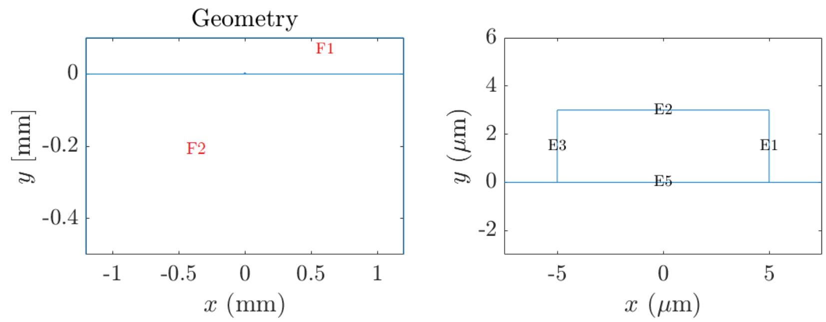

Figure 2: The geometry definition of the problem is shown in this figure. The region is divided into two subdomains (F1 and F2). In the equation of the problem statement, $(x, y < 0) = 12.9$ and $=$ 1 otherwise. The figure on the right is a zoomed-in version of the left figure emphasizing on the microstrip line.

Mesh formation

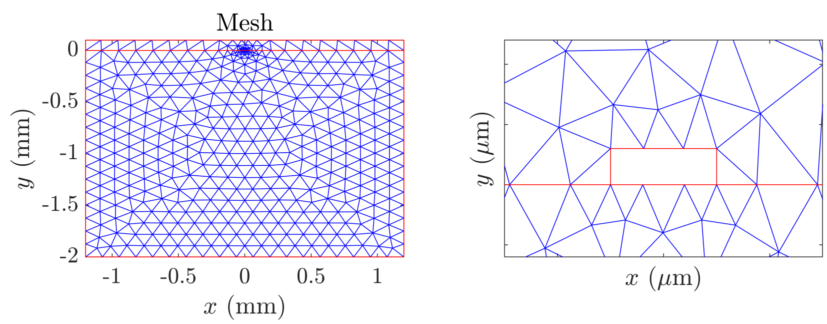

Figure 3: The mesh for the designated structure. The smallest inter-nodal distance is set to 25 % of 0.003 mm. The figure on the right shows the zoomed in picture of the microstrip.

In FEM method, the differential equation in Eqn. 1, on a domain delimited by $\Omega \subset \mathbb{R}^d$ is solved through dividing the entire domain into small triangular elements as seen in Fig. 3. These elements approximate the integrating function for the potential to be integrated over. We consider a 1st order approximation over our element, which means that the helper function is linearly varying over the element span.

$$\varepsilon_{xx} \frac{\partial^2}{\partial x^2} u + \varepsilon_{yy} \frac{\partial^2}{\partial y^2} u = 0 \tag{1}$$

Numerical Methodology

In solving the equation for FEM analysis, we convert the equation to weak form. In our case $\varepsilon_{xx} = \varepsilon_{yy} = \varepsilon$, piecewise constant on the two sub-domains, so the governing equation is $\nabla \cdot (\varepsilon \nabla u) = 0$. Multiplying by a test function $v(x, y)$ that vanishes on the boundaries where the potential is prescribed and integrating by parts,

$$-\int_{\Omega} \nabla \cdot (\varepsilon \nabla u)\, v \;\mathrm{d}\Omega = 0, \tag{2a}$$

$$\int_{\Omega} \varepsilon\, \nabla u \cdot \nabla v \;\mathrm{d}\Omega \;-\; \oint_{\partial\Omega} \varepsilon\, \frac{\partial u}{\partial n}\, v \;\mathrm{d}s = 0. \tag{2b}$$

Every boundary of the present problem (the strip perimeter and the outer box) carries a Dirichlet condition, so $v = 0$ on all of $\partial\Omega$ and the boundary integral vanishes, leaving $\int_{\Omega} \varepsilon \nabla u \cdot \nabla v \;\mathrm{d}\Omega = 0$. The dielectric interface at $y = 0$ is an internal edge and needs no explicit condition: continuity of $\varepsilon\, \partial u / \partial n$ across it is enforced naturally by the weak form.

The solution is approximated by the piecewise-linear (first-order) basis functions ϕ_i of the triangular mesh, $u = \sum_i U_i\, \phi_i$. Taking $v = \phi_j$ for every free node j yields the linear system

$$\sum_i K_{ji}\, U_i = 0, \qquad K_{ji} = \int_{\Omega} \varepsilon\, \nabla\phi_j \cdot \nabla\phi_i \;\mathrm{d}\Omega. \tag{3}$$

The matrix $\mathbb{K}$ is sparse: $K_{ji} \neq 0$ only when nodes i and j belong to a common triangle. On a triangle the gradients of the linear basis functions are constant, $\nabla\phi_i = [b_i;\ c_i]\,/(2A_e)$ with $b_i = y_j - y_k$ and $c_i = x_k - x_j$ $(i, j, k$ cyclic), so each element contributes in closed form

$$K_{ij}^{(e)} \;=\; \varepsilon_e\, A_e\, \nabla\phi_i \cdot \nabla\phi_j \;=\; \varepsilon_e\, \frac{b_i b_j + c_i c_j}{4A_e}, \tag{4}$$

where A_e is the element area and ε_e the relative permittivity of the sub-domain containing the element.

Formation and solution of the system of equations.

The potential throughout the domain is stored as a column vector with one row per mesh node. The global $\mathbb{K}$ is accumulated from the element contributions of Eqn. 4 as (row, column, value) triplets in a single sparse assembly (`fem_laplace2d.m`). The prescribed potentials enter the right-hand side by lifting: partitioning the nodes into free (F) and Dirichlet (B) sets,

$$\mathbb{K}_{FF}\, \mathrm{U}_F = -\,\mathbb{K}_{FB}\, \mathrm{U}_B \;\equiv\; , \tag{5}$$

where U_B holds the known values (5 V on the strip perimeter, 0 V on the outer boundary; the Laplace equation contributes no volume source). This reduced system is solved with MATLAB's sparse direct solver.

Results

Validation of the hand-assembled solver

The solver described above is implemented directly in MATLAB (`fem_laplace2d.m`, driver `FEM_handrolled_one_strip.m`) and validated against the MATLAB PDE Toolbox in three independent ways. The field plots of Figs. 4 and 5 were generated with the PDE Toolbox pipeline (`FEM_2D_one_strip.m`); the checks below show that this is numerically the same discretization as the hand-assembled solver.

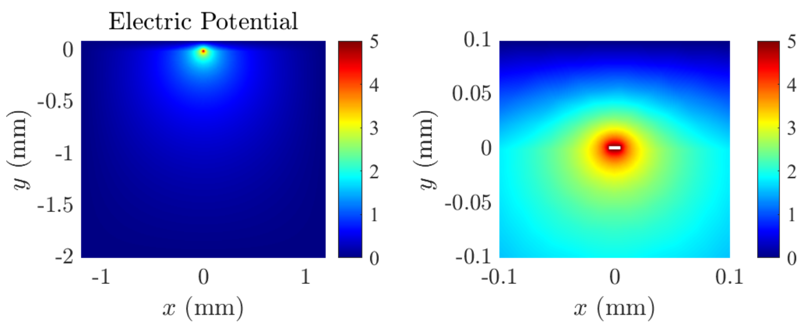

Figure 4: The potential profile distribution throughout the domain. (Left) The potential decays exponentially, and reaches close to 0, not far from the microstrip. (Right) A zoomed picture of the microstrip showing the potential decay.The potential on the microstrip is constant at 5 V. hence, It is not shown to avoid redundancy.

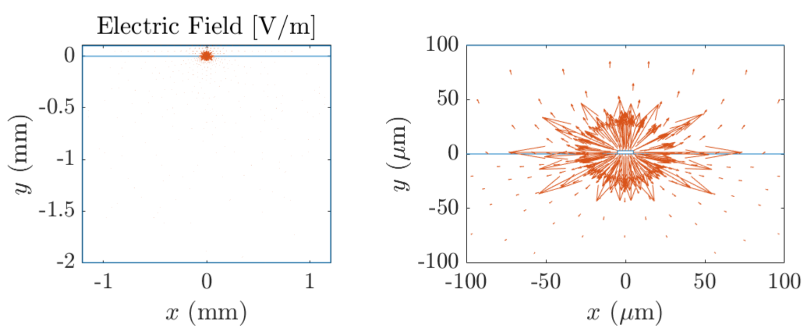

Figure 5: The electric field distribution of the domain. (Left) The electric field emanates outward radially from the microstrip. (Right) A zoomed picture of the microstrip showing the electric field magnitude decay. The field on the microstrip is non existent.

Same-mesh agreement. On every mesh of a uniform refinement sequence (536 to 128 936 nodes) the toolbox's own linear-element assembly (`assempde`) was run on the identical mesh with identical boundary conditions. The two solutions agree to $\max_i |\Delta u_i| \leq 2.3 \times 10^{-13}$ V, i.e. machine precision, confirming that the assembled stiffness matrix and the Dirichlet elimination are exactly the toolbox's linear FEM. Repeating the check on a mesh from the modern toolbox mesher (`solvepde` with linear elements, 14 705 nodes) gives 1.7×10^{-14} V.

Energy (capacitance) convergence. A pointwise error metric is a poor judge for this problem: the electric field is singular at the four corners of the strip (locally $u \sim r^{2/3}$ at the re-entrant 270° corners), so nodal differences near the strip are dominated by how each discretization resolves the singularity. The robust cross-check is the field energy $E_h = \frac{1}{2}\int_\Omega \varepsilon \, |\nabla u|^2 \, \mathrm{d}\Omega$, proportional to the line capacitance $C = 2\varepsilon_0 E_h / V^2$: for a Dirichlet problem the conforming-FEM energy converges to the true energy monotonically from above. Fig. 6 (right) shows the measured energy decrement ratios per refinement, 0.395–0.443, in close agreement with the theoretical $2^{-4/3} = 0.397$ for the corner singularity. Richardson extrapolation of the sequence gives $E_\infty = 98.07$ ($C = 69.5$ pF/m). The quadratic-element toolbox reference and the toolbox adaptive solver land 0.30 % and 0.10 % above E_∞ respectively, so all three discretizations agree on the capacitance to within a few tenths of a

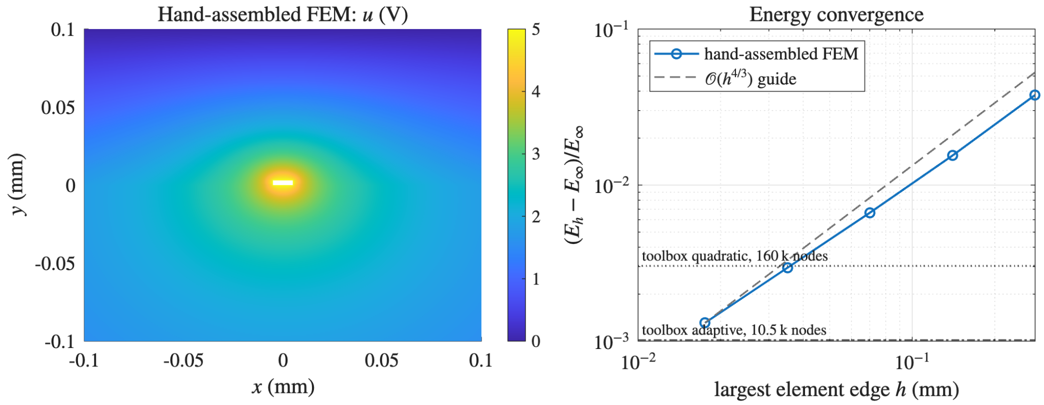

Figure 6: Validation of the hand-assembled solver. (Left) Potential computed by the hand-assembled FEM on the finest uniform mesh (128 936 nodes). (Right) Relative error of the field energy E_h with respect to the Richardson-extrapolated limit E_∞, versus mesh size. The convergence follows the $\mathcal{O}(h^{4/3})$ rate dictated by the $r^{2/3}$ field singularity at the strip corners. Horizontal lines mark the energies of two independent PDE Toolbox solutions: a quadratic-element reference (160 274 nodes, 0.30 % above E_∞) and the toolbox adaptive solver (10 473 nodes, 0.10 % above E_∞).

percent.

Pointwise comparison. On a fixed probe grid excluding 5 μm disks around the four corners, the hand-assembled solution differs from the quadratic reference by a few mV in the mid- and far-field. The largest differences, up to $\sim 4 \times 10^{-2}$ V ($\lesssim 1\,\%$ of the applied 5 V), are confined to the immediate $\sim$15 μm neighbourhood of the strip corners, where the corner singularity limits the pointwise accuracy of any fixed discretization (linear elements approach the corner field from below, quadratic elements from above).

Line parameters and closed-form benchmark

The electrostatic solution directly yields the transmission-line parameters of the structure. The stored field energy per unit length gives the line capacitance $C = 2\varepsilon_0 E_h / V^2$; repeating the solve with the dielectric removed ($\varepsilon = 1$ everywhere) gives C_0, and in the quasi-TEM approximation

$$\varepsilon_{\text{eff}} = \frac{C}{C_0}, \qquad Z_0 = \frac{1}{c\sqrt{C\,C_0}}. \tag{6}$$

Richardson extrapolation of the two energy sequences gives, for the Task 1 structure, $C = 69.5$ pF/m and $C_0 = 14.0$ pF/m, hence $\varepsilon_{\text{eff}} = 4.95$ and $Z_0 = 106.9\ \Omega$ (quadratic-element cross-check: $\varepsilon_{\text{eff}} = 4.99$, $Z_0 = 106.9\ \Omega$). The effective permittivity lies well below the $(\varepsilon_r + 1)/2 = 6.95$ of an open microstrip because the nearest ground of this structure is the cover only 0.097 mm above the strip, so a large share of the field energy resides in the air region. For the same reason open-microstrip closed-form models are not applicable to this shielded geometry, and a dedicated benchmark geometry is used instead to compare against the literature.

Closed-form benchmark. The same solver (`FEM_microstrip_benchmark.m`) was run on a standard open microstrip where the Hammerstad–Jensen model[1] applies: an $\varepsilon_r = 12.9$ substrate of height $h = 0.1$ mm with the ground plane at its bottom, a strip of width $W = 0.1$ mm ($W/h = 1$) and thickness $t = 2$ μm on top, and the side walls and cover pushed $30\,h$ away to emulate open space. Table 1 compares the Richardson-extrapolated FEM results with the closed form, including Hammerstad's strip-thickness correction. All three quantities agree to within 1 % — the stated accuracy class of the closed-form model itself — completing the quantitative validation of the solver against the literature.

Table 1: Hand-assembled FEM versus the Hammerstad–Jensen closed-form model for the benchmark microstrip ($\varepsilon_r = 12.9$, $W/h = 1$, $t/h = 0.02$).

	FEM	Hammerstad–Jensen	difference
ε_{eff}	8.40	8.48	$-1.00\,\%$
Z_0 (Ω)	42.83	42.72	$+0.24\,\%$
C (pF/m)	225.7	227.4	$-0.74\,\%$

Task 2

Through the same methodology, Task 2 has been performed, except with an extra set of inner boundaries having Dirichlet conditions $u = -5$ V.

Methodology - Domain Discretization and Mesh formation

The geometry description and the meshed domain figure are shown below. From the geometry, we can identify the inner and outer boundaries. They are listed below: **Inner boundaries:**

- E1 $\longrightarrow$ 5
- E2 $\longrightarrow$ 5
- E6 $\longrightarrow$ 5
- E8 $\longrightarrow$ 5
- E3 $\longrightarrow$ -5
- E4 $\longrightarrow$ -5
- E7 $\longrightarrow$ -5
- E10 $\longrightarrow$ -5

Results - Solution of SOEs

The results obtained for the two microstrip problem are shown below.

[1] E. O. Hammerstad and Ø. Jensen, "Accurate models for microstrip computer-aided design," *IEEE MTT-S Int. Microwave Symp. Digest*, 1980, pp. 407–409.

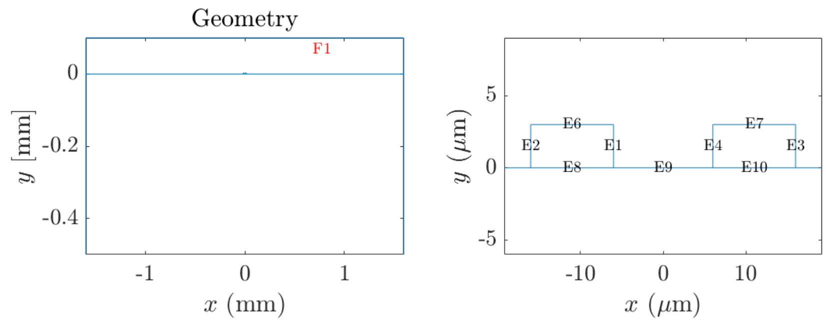

Figure 7: The geometry definition of the second task is shown in this figure. The region is divided into two subdomains (F1 and F2). In the equation of the problem statement, $(x, y < 0) = 12.9$ and $= 1$ otherwise. The figure on the right is a zoomed-in version of the left figure emphasizing on the microstrip line.

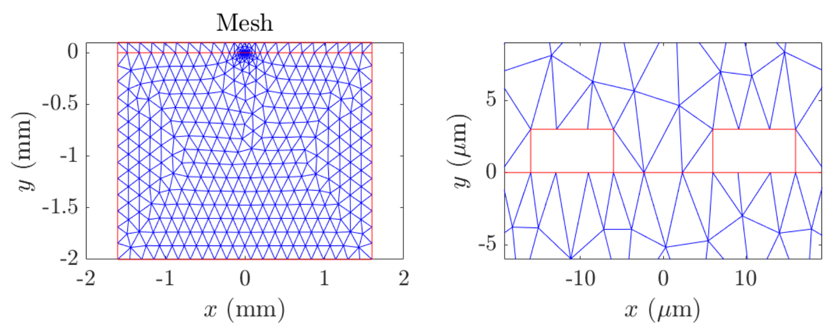

Figure 8: The mesh for the designated structure. The smallest inter-nodal distance is set to 25 % of 0.003 mm. The figure on the right shows the zoomed in picture of the microstrip.

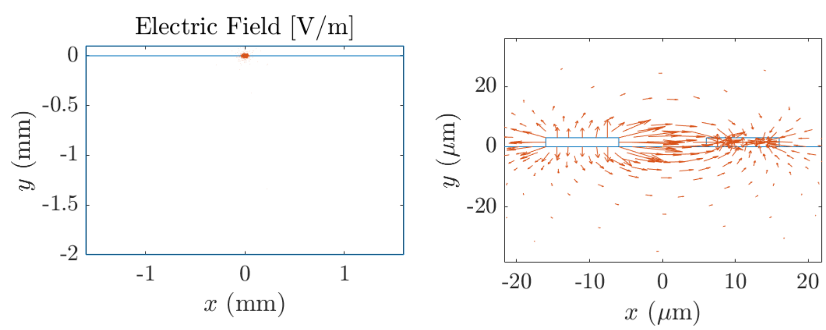

Figure 10: The electric field distribution of the domain. (Left) The electric field emanates outward radially from the left microstrip and ends at the left microstrip. (Right) A zoomed picture of the microstrip showing the electric field magnitude decay. The field in the microstrip is non existent.

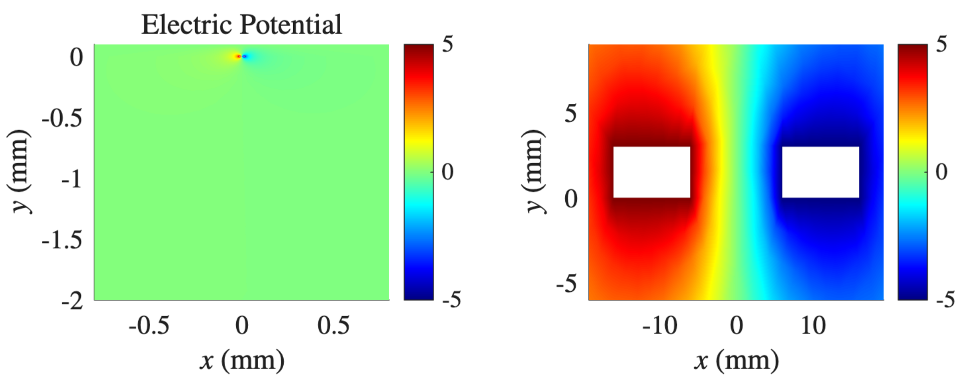

Figure 9: The potential profile distribution throughout the domain. (Left) The potential decays exponentially, and reaches close to 0, not far from the two microstrips. (Right) A zoomed picture of the microstrip showing the potential decay. The potential on the left microstrip is constant at 5 V and that on the right microstrip is -5 V.